Available online at www.sciencedirect.com
SCIENCE DIRECT®
Solid State Sciences 8 (2006) 740–752
Solid State Sciences
www.elsevier.com/locate/ssscie

Towards enumeration of crystalline frameworks: the 2D hyperbolic approach

S.T. Hyde [a,*], O. Delgado Friedrichs [b], S.J. Ramsden [a], V. Robins [a]

[a] *Department of Applied Mathematics, Research School of Physical Sciences, The Australian National University, Canberra ACT 0200, Australia*
[b] *Department of Chemistry and Biochemistry, Arizona State University, Tempe, 85287 AZ, USA*

Received 11 January 2006; received in revised form 30 March 2006; accepted 18 April 2006

Available online 5 June 2006

Abstract

Crystalline frameworks in 3D Euclidean space can be constructed by projecting tilings of 2D hyperbolic space onto three-periodic minimal surfaces, giving surface reticulations. The technique involves Delaney–Dress tiling theory, group theory, differential and non-Euclidean geometry. Preliminary results of this approach, found at http://epinet.anu.edu.au, are discussed and compared with other approaches.

PACS: 61.50.Ah; 89.75.Hc; 02.20.-a; 02.40.-k

Keywords: Hyperbolic tilings; Minimal surfaces; Networks; Frameworks; Reticular chemistry; Symmetry groups

1. Introduction

Crystalline structures in solid-state chemistry are a wondrous playground for geometers and topologists. The role of geometry in atomic and molecular ordering in the solid state can hardly be exaggerated. Kepler's observations of snowflakes were intricately related to his studies of Archimedean polyhedra. In a similar vein, Haüy explained the characteristic angles between crystal faces in terms of polyhedral atomic building blocks, thereby formulating his Law of Rational Indices. The concepts of topology, in its infancy in the latter half of the nineteenth century, lay at the heart of Crum Brown's conceptual advances in organic and solid state chemistry. Crum Brown proposed a simple graph theoretic notation for molecular topology (that led at once to the concept of molecular isomerism [1]). He maintained a life-long interest in knots and weavings, inspiring the development of knot theory (kicked off in spectacular fashion by his mathematical brother-in-law, Tait). In 1883, Crum Brown constructed an astonishingly modern framework model describing the mutual arrangement of Na and Cl atoms in crystalline NaCl, built from balls of colored wool and knitting needles [2], perhaps the first network model of solids. The framework model described both the bonding topology of NaCl (now passé) and the relative geometry of Na and Cl atoms, thereby revealing the inherent symmetry in a crystal of NaCl. Von Laue's discovery in 1912 of the diffraction of X-rays when traversing crystals unequivocally demonstrated the relevance of symmetrical patterns to crystals, giving birth to the science of crystallography. The fundamental connection between geometry and crystal science—evident to Kepler, Haüy and Crum Bown—has been present since the earliest days of crystallography.

Thanks to instrumental developments over the past century in X-ray, electron and synchrotron optics, solid state structural science has undergone a spectacular growth in our understanding of crystalline material structures, from modulated crystal structures, to quasicrystalline materials. However, this data explosion has *not* been matched by increased awareness of modern mathematical approaches to structure. Non-Euclidean and differential geometry, topology and discrete mathematics have matured considerably in past decades. Yet we remain unable to answer some simple questions relevant to chemical structure. One such question is the following: what are the topological constraints on three-dimensional periodic networks? For example, what variety of ring-sizes are allowed from a four-connected network? Such questions have so far resisted simple answers; our best hope is to attempt systematic enumeration of crystalline frameworks (or *crystal nets*).

* Corresponding author.
E-mail address: stephen.hyde@anu.edu.au (S.T. Hyde).

1293-2558/$ – see front matter
doi:10.1016/j.solidstatesciences.2006.04.001

Three-dimensional framework models—visionary in Crum Brown's day—have proven to be fruitful ground for structural chemists since. These models are widely used descriptions of three-dimensional structure in chemistry [4]. Among many contributors, comprehensive investigations into crystal nets are those of Wells [3] and, more recently, O'Keeffe and colleagues [4,5]. The advent of graph theoretic concepts [6,7] and Delaney–Dress tiling theory [8–10] has allowed chemists to move beyond empirical catalogues. Frameworks—mathematical *graphs*—are intrinsically one-dimensional structures. Their spatial embeddings, defined by the geometrical locations of framework vertices, define three-dimensional volumes that tile space. These tiles are occasionally plane-faced polyhedra, but, more commonly, they are cells with curved saddle-shaped surfaces, resembling the *saddle polyhedra* that were systematically studied by Pearce [11].

Wells also realised the importance of moving beyond plane-faced polyhedra [3]. He introduced to chemists the concept of *infinite polyhedra*, described earlier by Coxeter (who derived the three regular infinite polyhedra with his friend Petrie while both were schoolboys [12]). Whereas conventional (convex) polyhedra are topological spheres and stellated polyhedra are multiple coverings of the sphere, the sponge-like forms of infinite polyhedra are hyperbolic surfaces of infinite genus. There remains an interesting duality between crystal nets and infinite polyhedra exploited in detail in this paper.

Consider, for example, Crum Brown's network model of NaCl: nodes disposed in a simple cubic arrangement in 3D Euclidean space ($\mathbb{E}^3$) with edges connecting nearest neighbour nodes to form a *regular* network with symmetrically equivalent edges and degree-six vertices (6-valent, 6-connected, 6-coordinated). This primitive cubic network is called *pcu* by O'Keeffe [13]. How this structure is described is dependent on the viewer. To Crum Brown, it appeared more or less as shown in Fig. 1. To graph theorists and some crystallographers, [6,14–16], it is an infinite graph, readily described by its *quotient graph* (the graph formed by identifying all equivalent edges and vertices displaced by translations of the lattice), shown in Fig. 2. Labelling the displacements along directed edges in terms of a translation vector (i, j, k) identifies the periodic net up to isomorphism.

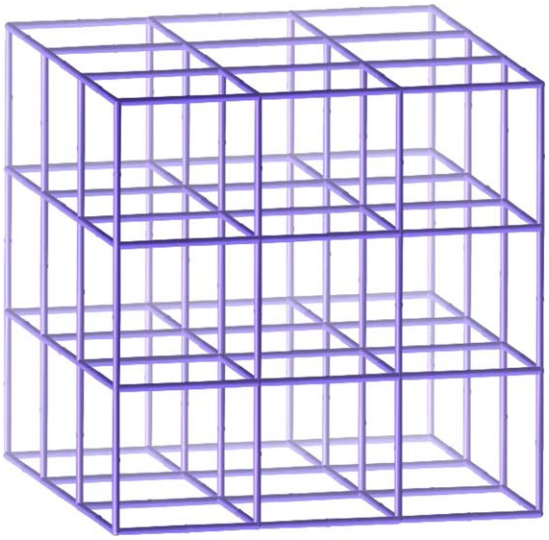

Fig. 1. A stick model of the *pcu* (primitive cubic) crystal net.

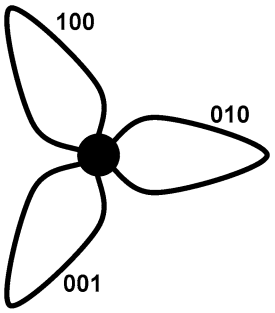

Fig. 2. Quotient graph of the simple cubic crystal net.

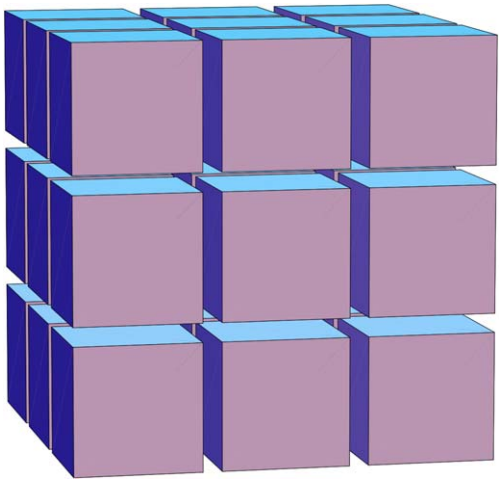

Fig. 3. The *pcu* net carried by cubic natural tiles.

Alternatively, the *pcu* crystal net consists of the edges of a tiling of 3D Euclidean space by face-sharing cubes, illustrated in Fig. 3. This description decomposes the volume into *natural tiles*, of maximal point group symmetry [10] and the *pcu* net is carried by the edges of the tiling. We note that many alternative cellular decompositions are possible for any given crystal net. This approach can be combined with Delaney–Dress tiling theory to give a systematic constructive algorithm for crystal nets and their duals (defined with respect to the natural tiling decomposition) up to any desired degree of complexity. A canonical signature and geometric realisation of these crystal nets is achieved using the *Systre* software package [17], part of the larger *GAVROG* package of Delgado Friedrichs [18]. The topological part of the procedure determines the smallest primitive cell for the crystal net and its combinatorial symmetries then furnish a unique label which we call the *Systre key*. The algorithm is based on computing a barycentric placement for the net where each vertex lies at the center of mass of its neighbours. The geometric realisation is made by finding a metric that realises the combinatorial affine symmetries as Euclidean isometries.

A third perspective—the topic of this paper—adopts yet another interpretation of the *pcu* crystal net. Here the *pcu* net is

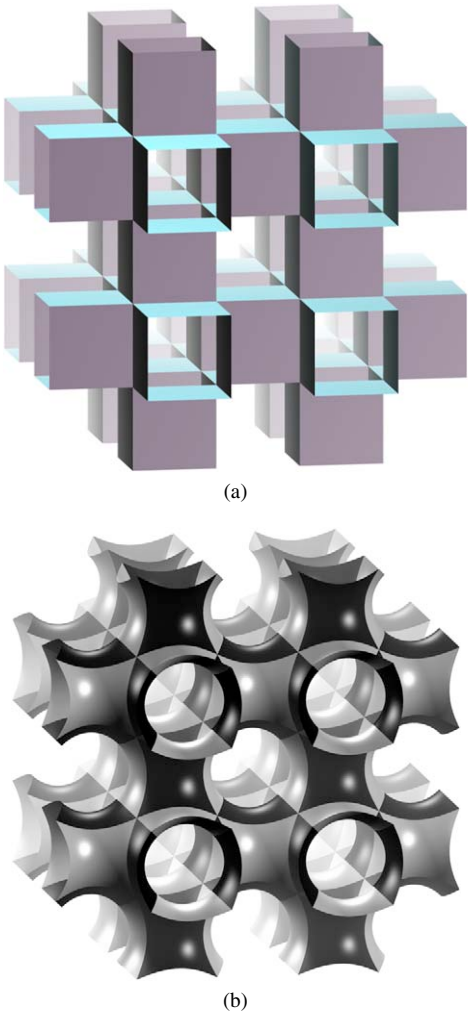

Fig. 4. (a) The *pcu* net is carried by edges of a single regular infinite $\{4, 6\}$ polyhedron, a sponge-like cell of infinite genus. (b) The polyhedron is relaxed to obtain a smoothly-curved three-periodic minimal surface (the P surface). Adjacent faces are coloured alternately grey/black to highlight distinct faces.

'carried by' a pair of interpenetrating sponge-like tiles. Each tile consists of an infinite number of fused cubes, forming a three-dimensional array illustrated in Fig. 4. This tile is one of Coxeter's regular infinite polyhedra, with symmetrically identical vertices, edges and faces [12]. Just two of these tiles are needed to tessellate the whole of space; these 3D tiles are separated by a three-periodic hyperbolic surface. The surface shared by each infinite tile has six square faces incident to each vertex and so within this surface perspective, the *pcu* net has Schläfli symbol $\{4, 6\}$. A generic $\{n, z\}$ tiling can be realised as a regular tessellation of the sphere, Euclidean plane or hyperbolic plane, depending on whether the product $(n - 2)(z - 2)$ is less than, equal to, or greater than four, respectively. The regular $\{4, 6\}$ net—with symmetrically identical $\{4\}$ faces, edges and vertices—is therefore a tiling of the hyperbolic plane, revealing the 2D hyperbolic nature of this perspective of the *pcu* net.

It is mathematically most convenient to relax the plane-faced infinite polyhedron and anneal out the edge creases, so that the all faces have zero mean curvature everywhere, making the smoothed infinite polyhedron a *minimal surface*, also illustrated in Fig. 4. Minimal surfaces, characterised by vanishing mean curvature and variable Gaussian curvature, are the simplest generalisation of plane-faces to curved ones. They are everywhere saddle-shaped, with equal and opposite principal curvatures, i.e., saddles of equal convexity along one tangential direction on the surface and concavity in the orthogonal direction.

Our view of the *pcu* net is therefore not based on the Euclidean geometry of planar squares, or cubes, but on the hyperbolic geometry of a three-periodic minimal surface described in the following sections. The crystal net is a *surface reticulation*, where the surface is the domain wall of an infinite bicontinuous 3D tiling of space. Our enumeration of crystal nets proceeds via an enumeration of hyperbolic tilings that are compatible with a given minimal surface.

2. Crystal nets from hyperbolic tilings

The enumeration and study of three-periodic minimal surfaces is a problem in differential geometry and complex analysis, but it has been developed largely in response to the recognition of their importance in describing complex crystal structures by Andersson and colleagues [19–22]. Hans-Georg von Schnering has been associated with this work from its earliest days and must be credited for his enthusiastic support of the approach. Together with Nesper, he developed simple level surface expressions involving the circular trigonometric functions for three-periodic hyperbolic surfaces, whose topology mimics that of the three-periodic minimal surfaces [23].

The simplest three-periodic minimal surfaces are those with a unit cell associated with a genus-three torus (a three-holed donut). The association is made by identifying faces of the unit cell according to its lattice vectors to form a boundary-free *compact* surface. Five three-periodic genus-three minimal surfaces exist: the P, D, G, H and CLP surfaces: other genus-three examples are lower-symmetry variants of these cases [24,25]. For each of these five surfaces, we have found a symmetry-preserving *covering map* that wraps the hyperbolic plane onto the surface, in much the same way the Euclidean plane wraps onto a cylinder, as shown in Fig. 5.

To enumerate surface reticulations, we first enumerate hyperbolic tilings with symmetries that are compatible with the unit cell translational symmetries. This ensures that (i) the tilings are commensurate with the surface—when wrapped up, the copies lie exactly on top of one another and (ii) the translational symmetries of the reticulation are identical to those of the oriented surfaces (whose front and back sides of faces are coloured differently). The latter constraint is unnecessary, but imposes a convenient limit on the complexity of the net catalogue. A complete enumeration of symmetries compatible with the orientation-preserving translations of the P, D, and G surfaces is given in [26]. To obtain the hyperbolic tilings we apply Delaney–Dress tiling theory to the 2D hyperbolic plane: that theory allows for exhaustive construction of all tilings of a given symmetry group up to an arbitrary number of vertices (or faces) per asymmetric domain.

To date, we have enumerated a special subset of reticulations of the P, D and G surfaces: those arising from symmetry

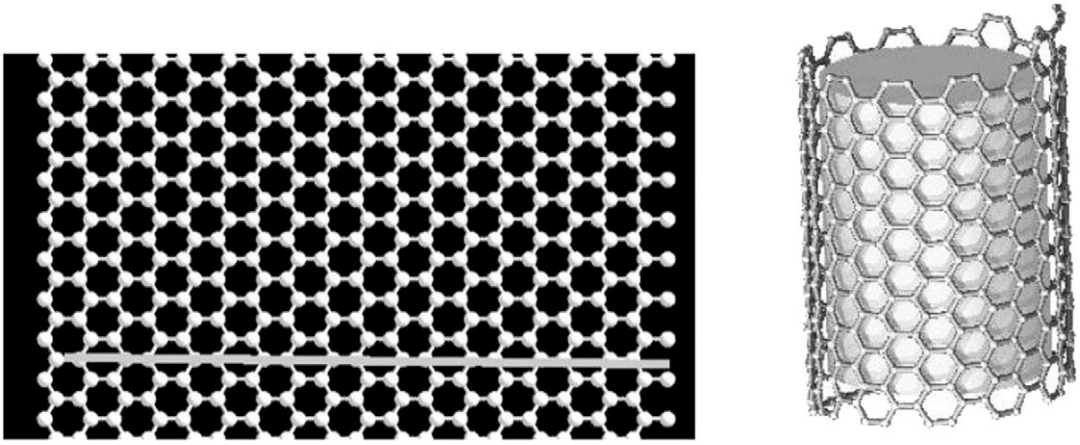

Fig. 5. Mapping the Euclidean {6, 3} net to the cylinder: the graphite network is rolled, gluing ends of the equatorial line. The length and orientation of that line determines the tubule radius and chirality respectively. (Tubule image courtesy of D. Tomanek.)

groups defined by reflections only (the *kaleidoscopic* or *Coxeter* groups). We have also limited the enumeration of hyperbolic tilings to those containing up to two symmetrically distinct vertices or tiles. In the jargon of Delaney–Dress tiling theory; these include vertex-1- and vertex-2-transitive and tile-1- and tile-2-transitive tilings respectively. The following section discusses the results of this enumeration in detail.

3. Epinet: Euclidean patterns from non-Euclidean tilings

Three distinct stages are used in our EPINET enumeration of crystal nets: hyperbolic tilings, surface reticulations, and canonical barycentric embedding. Preliminary results of our EPINET crystal net enumeration are now available at http://epinet.anu.edu.au [27].

The first step involves only the 2D intrinsic geometry of the P, D, and G surfaces. We decorate fundamental domains of the 2D hyperbolic group with edges and vertices in a systematic fashion, governed by the constructive algorithms of Delaney–Dress tiling theory. That decoration produces tilings of the 2D hyperbolic plane, $\mathbb{H}^2$. The tilings are labelled according to their 2D hyperbolic group (viz. their Conway orbifold symbol [28]) and the tile class according to Delaney–Dress tiling theory (F for fundamental, G for glued, S for split [29]). For example, the most symmetric hyperbolic kaleidoscopic group that is commensurate with all translational symmetries of the P, D, and G surfaces is described by the ⋆246 orbifold. The fundamental tiling within that symmetry gives rise to a tiling of $\mathbb{H}^2$ labelled as ⋆246_F_1 (see http://epinet.anu.edu.au/hqc265). The edge skeletons of these tilings are hyperbolic networks that we call h-nets.

The hyperbolic nets are wrapped onto the P, D, and G surfaces, giving three-periodic surface reticulations, called e-nets. The wrapping of $\mathbb{H}^2$ onto the P, D and G surfaces is realised by aligning the special symmetry sites of the tiling with related sites on the surfaces. Indeed, the $\mathbb{H}^2$ tilings are multiple (infinite) covers of these surfaces and judicious choice of hyperbolic groups ensures that the multiple covers result in a unique copy on the surface, described above. (This is directly analogous to the process of projecting planar 2D crystalline tilings onto the surface of a cylinder, forming one-periodic cylindrical reticulations.) The e-nets therefore lie in the relevant minimal surface. We can identify all intrinsic 2D features of e-nets, including their hyperbolic symmetries and sizes of rings on the surface, from the h-net. Note that there is a one-to-one correspondence between the hyperbolic symmetry of the h-net and the resulting 3D Euclidean space group symmetry of the e-net. The relations between the hyperbolic 2D and Euclidean 3D groups for the reticulations are listed at http://epinet.anu.edu.au/pgd_subgroups/list.

In moving from a tiling to its associated net, we ignore some of the symmetries encoded by the Delaney–Dress symbol. This means that different hyperbolic tilings can generate the same e-net. The surface reticulations are therefore filtered to determine those e-nets with distinct topologies, and then listed in order according to their genus-three Delaney–Dress symbol. We give each distinct e-net a label of the form $eqcN$ where the q is replaced by p, d, or g depending on the surface reticulated, and the c stands for 'Coxeter' hyperbolic symmetry group. The integer N runs from 1 to 5912, so the total number of e-nets is 3×5912, one on each of the three surfaces. Our example above, the tiling ⋆246_F_1 wraps onto the P surface to give the e-net epc5701, viewable at http://epinet.anu.edu.au/epc5701.

Finally, the e-nets are symmetrised as far as possible by calculating barycentric embeddings of the reticulation topologies, using *Systre*, to give s-nets. Continuing with our example, the ⋆246_F_1 tiling wrapped onto the P surface gives the s-net sqc12642, online at http://epinet.anu.edu.au/sqc12642. Here s denotes the *Systre* process for barycentric embedding, q indicates that the crystal net was derived by a reticulation of a cubic (q-*bic*) three-periodic minimal surface (namely the P, D, G family), c again denotes a Coxeter group, and the number (12 642) is a sequential integer between 1 and 14 532.

It is possible for different e-nets to give the same s-net, either through reticulations on different surfaces, or from reticulations with different unit cells on the same surface. Thus, there are fewer s-nets than e-nets and the ordering of s-nets is via their systre key (a canonical form of the quotient graph obtained via

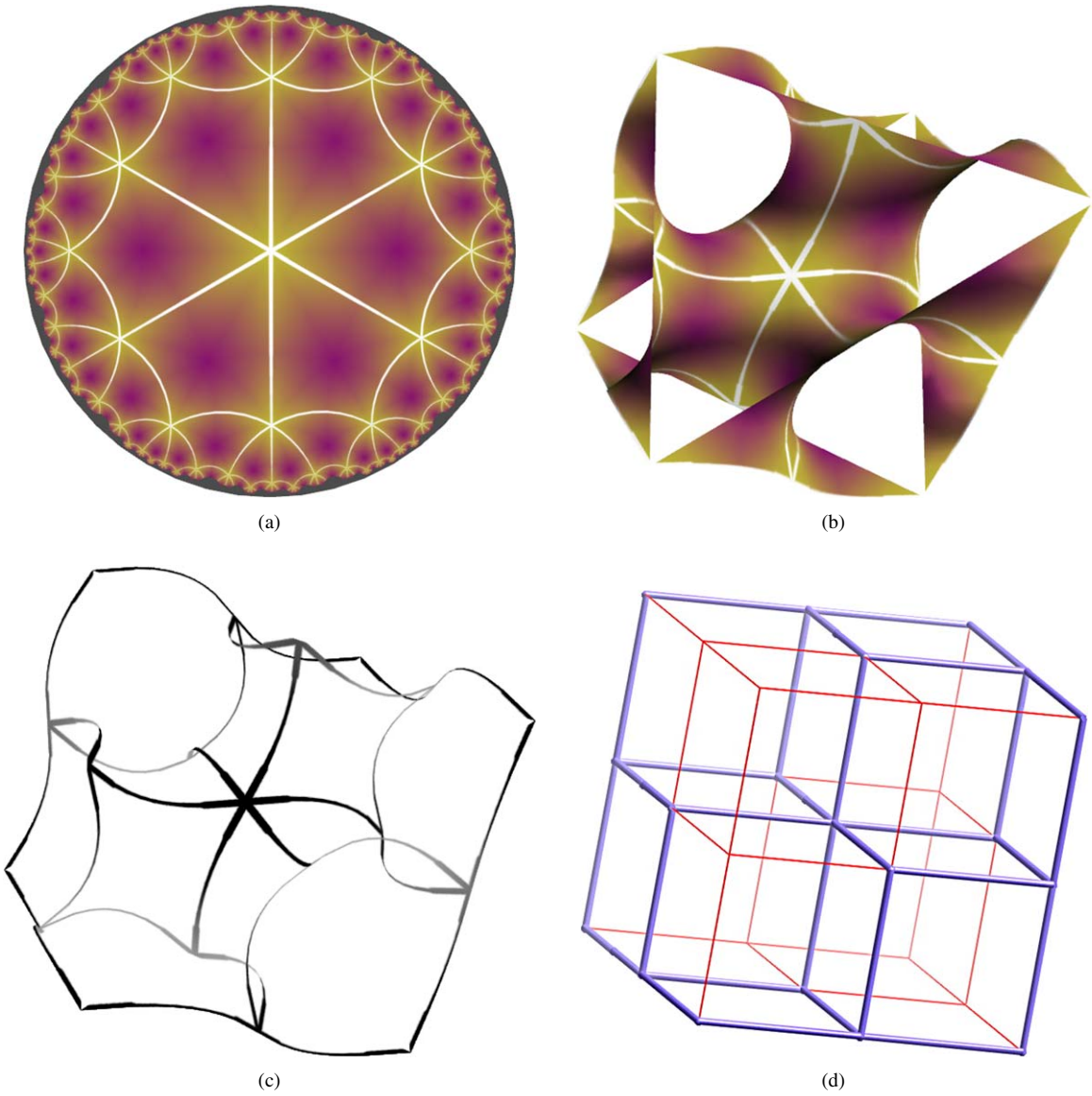

Fig. 6. (a) A Platonic tiling of $\mathbb{H}^2$ with six hyperbolic squares per vertex, $\{4, 6\}$. The resulting h-net is drawn in the Poincaré disc model of $\mathbb{H}^2$, shaded to reveal the kaleidoscopic symmetry of the tiling. (b) Surface reticulation of the $\{4, 6\}$ h-net onto a fragment of the P minimal surface. (c) The resulting e-net, and (d) its barycentric embedding, the s-net labelled *sqc*1, identical to *pcu* (with unit cell edges outlined in red).

the barycentric embedding process). This sort induces a natural hierarchy of networks by net topology and symmetry.

Our enumeration of nets will expand in the future to include non-kaleidoscopic 2D tilings on the P, D, and G surfaces, then further to reticulations of other three-periodic minimal surfaces. The labels for the e- and s-nets will reflect this: the q label will change according to the surface, and the c label will be replaced by tags for other orbifold classes.

The relationship between e- and s-nets is somewhat subtle. Typically the s-net is a simple deformation of the e-net that involves no edge crossings (i.e., they are *ambient isotopic*), but in some cases changes in topology and embedding occur. For example, two edges may coalesce, described further below. The distinction between e- and s-nets is a useful one to retain since the e-nets formed by surface reticulations may encode double bonds and *knotted crystal nets*, of increasing relevance to metal-organic frameworks (*MOFs*), discussed below.

These details are best illustrated by examples. We have seen that the *pcu* crystal net can be carried by a $\{4, 6\}$ infinite regular polyhedron in 3D Euclidean space ($\mathbb{E}^3$). The same tiling can be embedded in the hyperbolic plane as a regular h-net, forming a kaleidoscopic pattern (with $\star 246$ orbifold), shown in Fig. 6. That pattern can be projected into $\mathbb{E}^3$ by wrapping onto the P surface, forming an e-net, with curved edges (Fig. 6). Barycentric embedding of this e-net gives the s-net *sqc*1, whose *Systre key* matches that of the *pcu* net.

Note that the topology of h-net antecedents of *pcu* need not be confined to $\{4, 6\}$: other combinations of circuits are present in the *pcu* net that can form the basis of an h-net that projects to the *pcu* net. In other words, the projection from $\mathbb{H}^2$ to $\mathbb{E}^3$, from a source h-net to the target s-net, is many-to-one: other h-nets

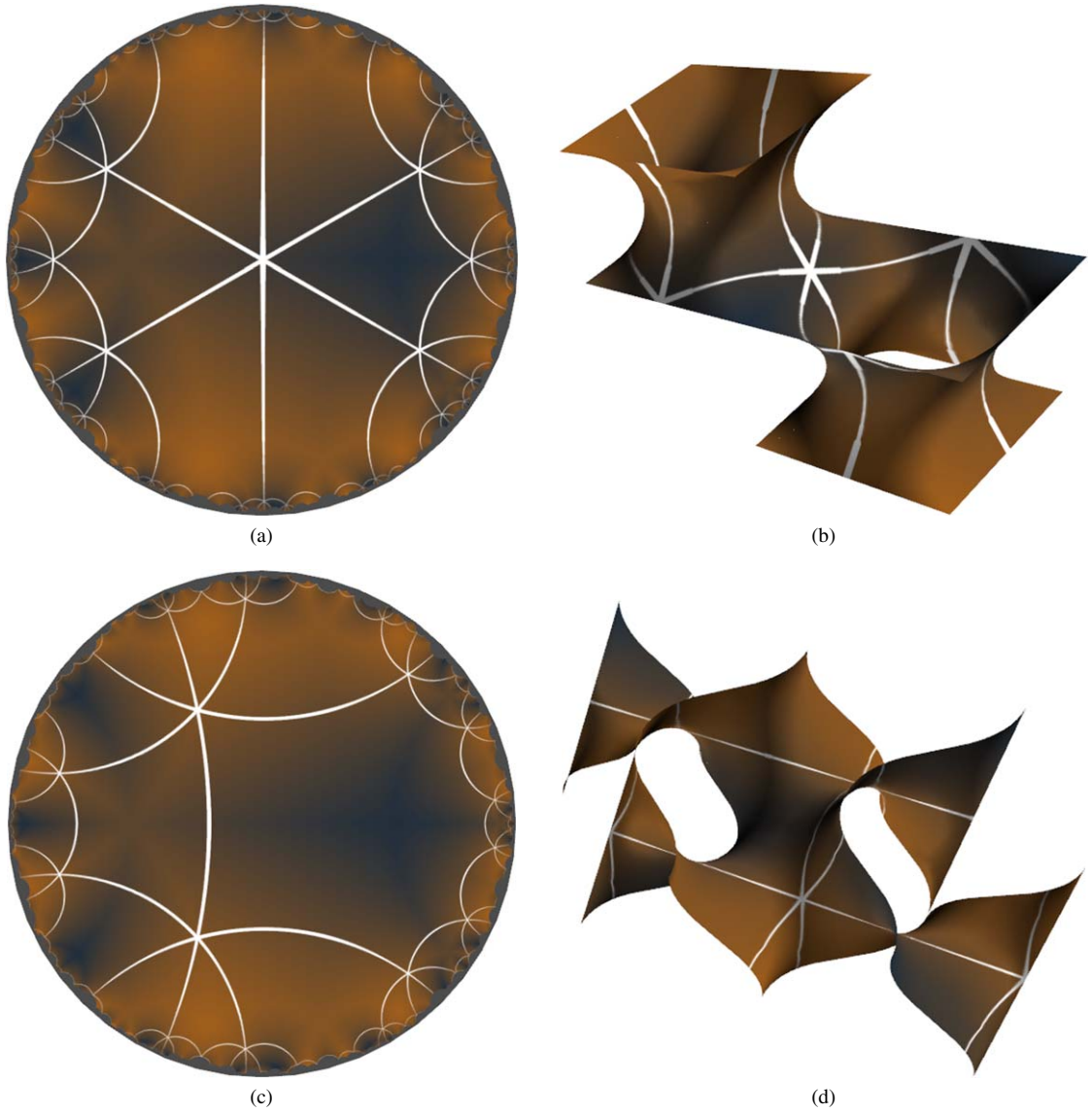

Fig. 7. Wrapping of (4.8.8.4.8.8) tilings of $\mathbb{H}^2$ to form the *pcu* net with six hyperbolic squares per vertex, {4, 6}. (a), (c) Alternative locations of the *h*-net in $\mathbb{H}^2$, both with orbifold symmetry ⋆4444. (b), (d) Wrapping of the *h*-nets onto the *P* and *D* surfaces respectively, to give tetragonal and orthorhombic surface reticulations (*e*-nets). Both *e*-nets give the *pcu* crystal net after barycentric embedding.

and *e*-nets also relax to the *sqc*1 net (these are listed as *Source Tilings* at http://epinet.anu.edu.au/sqc1). For example, the *h*-net with 2D Schläfli symbol (4.8.8.4.8.8) can be wrapped onto the *P* and *D* surfaces to also give *pcu*, as shown in Fig. 7.

In all cases, the topology of the *h*-net is conserved under projection from $\mathbb{H}^2$ to $\mathbb{E}^3$ to form the *e*-net, with all cycles of the *h*-net preserved as surface rings (null-homotopic cycles) of the reticulation. The surface wrapping of $\mathbb{H}^2$ onto the three-periodic minimal surfaces induces extra 'collar'-rings in the *e*-net, of non-trivial surface homotopy. Subsequent relaxation from the *e*-net to the *s*-net may result in multigraphs, with more than a single edge joining two vertices. This occurs, for example, when a pair of edges surrounds a channel of the surface, giving a two-edge collar-ring. We merge these multiple edges into a single edge in the *s*-net, identifying these examples in EPINET as *non-vertex degree preserving* examples (e.g., Fig. 8).

3.1. 2D vs. 3D crystallographic nature of epinets

Results of the crystal net enumeration are difficult to summarise on paper, hence the EPINET site, that collects *h*- and *e*-nets under the *2D Tilings* entries on EPINET, and *s*-nets under the *3D Networks* entries. The *s*-nets are illustrated as 3D VRML images, with arbitrary metric (i.e., all cells are unit cubes). They are also represented by a more conventional crystallographic (*CrystalMaker*) drawing that utilises the *Systre* refinement of the cell parameters. Those parameters, plus vertex sites and edges, are tabulated on the site. Due to limitations of the *CrystalMaker* software [30], we cannot guarantee the fidelity of these drawings in all cases, particularly where long bonds are present (described below). We hope to rectify this in the near future, via an extension of the software capabilities.

In many cases, *s*-nets found by our algorithm embed in $\mathbb{E}^3$ to form strikingly Euclidean patterns, despite their non-

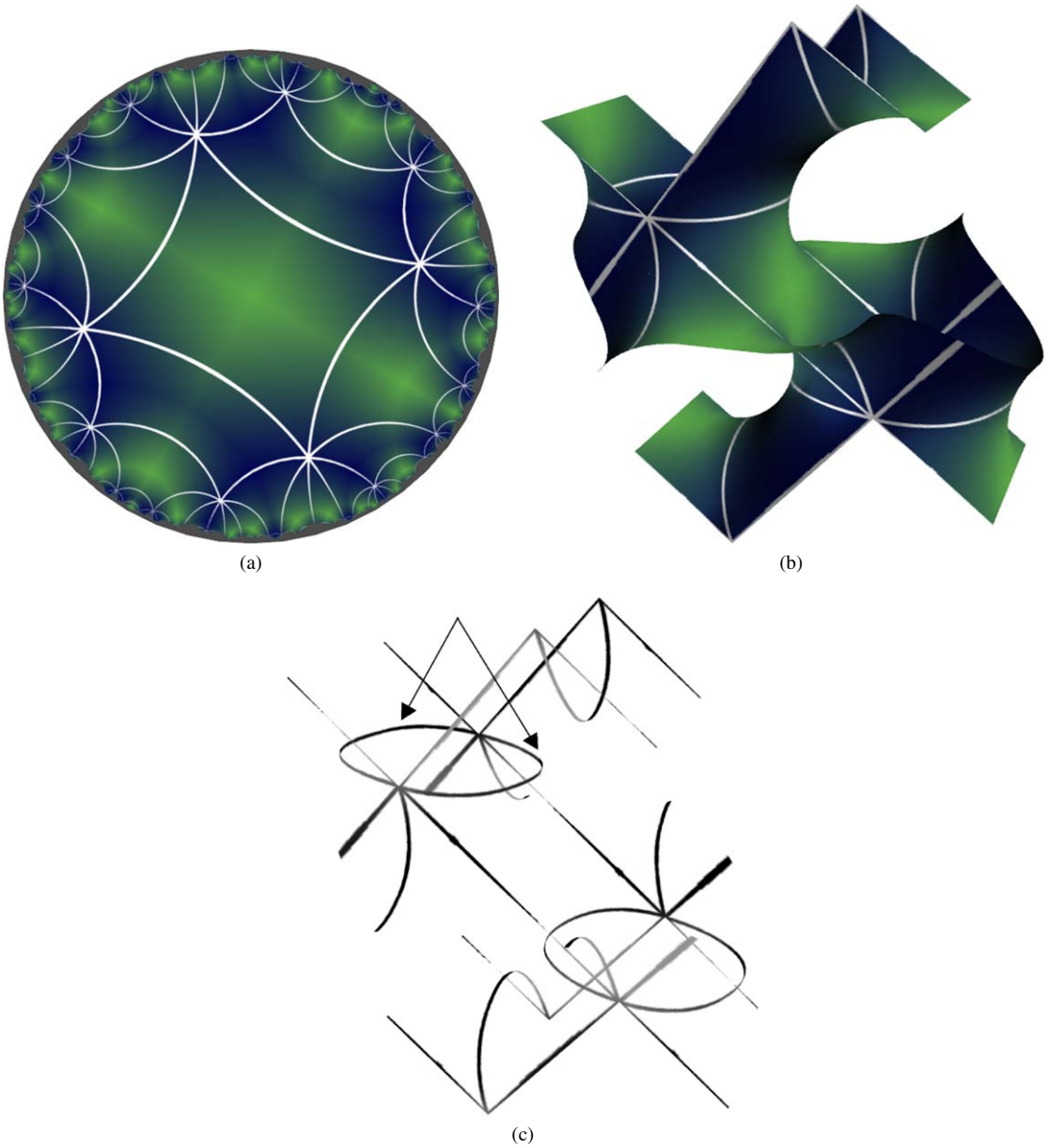

Fig. 8. The $(4, 12)$ tiling of $\mathbb{H}^2$ wraps onto the P surface to form the *pcu* net. (a) The $(4, 12)$ tiling of $\mathbb{H}^2$ with orbifold symmetry ⋆2222. (b) Wrapping the tiling onto the P surface. (c) The resulting e-net whose barycentric embedding is also the *pcu* crystal net. Edges in a collar-ring of size two are marked by arrows. This collar collapses to a single edge in the barycentric embedding.

Euclidean origins. These examples remind us that we see frameworks through the lens of our prior experience. For example, though the *sqc*12217 pattern in Fig. 9 emerges from a degree-5 (6.3.3.3.6) h-net, the resulting s-net is most readily identified as an array of Platonic octahedra, joined by single edges.

Perhaps the simplest cases to analyse are the crystal nets that arise from triangulations of the hyperbolic plane, viz. $\{3, z\}$ networks (where z exceeds 6). Just as the regular $\{3, 6\}$ network represents close-packing of circular discs in the Euclidean plane, regular $\{3, z\}$ h-nets represent close-packed 2D hyperbolic discs. The current enumeration gives 9 distinct s-nets, of which 3 are made of arrays of Euclidean equilateral triangles. The examples are listed in Table 1.

We have confined our results to date to kaleidoscopic orbifolds only, so that all h-nets contain 2D asymmetric domains bounded exclusively by mirror lines in $\mathbb{H}^2$. Since our enumeration is constrained to patterns whose hyperbolic groups respect all translations of the underlying surface (whose sides facing 'inner' and 'outer' volumes are colored distinctly), unit cells of the e-nets conform to those of the oriented surfaces (i.e., excluding translations that reverse the sides of the surface). Fig. 10 displays the distribution of space groups of all e-nets formed by projections of h-nets with one or two types of tile, and (their 2D duals) one or two types of vertex. All crystal classes except triclinic and hexagonal are found in the e-nets. Triclinic cases are not formed due to the restriction to kaleidoscopic groups: we expect examples to appear in enumerations

Fig. 9. The cubic crystal net *sqc*12217, a 5-coordinated sphere packing ($5/3/c10$ [31]), labelled by O'Keeffe as *crs-a* or *dia-h* [13].

Table 1
Barycentric embeddings in $\mathbb{E}^3$ (s-nets) derived from hyperbolic triangulations, $\{3, z\}$ wrapped onto the P, D, or G minimal surfaces

2D Schläfli	Surface	s-net	Space group	No. nodes	Equal edges
{3, 8}	P	*sqc*5309	$I4/mmm$	2	Yes
	G	*sqc*10878	$I4_1/acd$	2	No
	D	*sqc*5051	$P4_2/nnm$	2	No
	P	*sqc*5115	$I432$	1	No
	G	*sqc*10983	$I4_132$	1	No
	D	*sqc*10956	$Fd\bar{3}m$	1	Yes
{3, 9}	P	*sqc*2580	$I432$	1	No
	G	*sqc*8558	$I4_132$	1	No
	D	*sqc*8843	$Fd\bar{3}m$	1	Yes

The EPINET label, space groups, and number of nodes per asymmetric unit are listed. Those s-nets with all edges of equal length—forming nets with equilateral Euclidean triangles—are also flagged.

of crystal nets from hyperbolic patterns with non-kaleidoscopic symmetries. Hexagonal examples are excluded due to the restriction to the PDG surface family. Hexagonal e-nets will emerge from reticulation of the (hexagonal) H three-periodic minimal surface [32].

Barycentric embeddings of the e-nets give the s-nets, whose space groups are usually super-groups of the corresponding e-nets. The resulting distribution of symmetries is shown in Fig. 11. Comparison of Fig. 10 and Fig. 11 confirms that embedding with barycentric coordinates lifts the symmetry.

It is of some interest to compare the vertex transitivity of the s-nets with those of the h-nets. The distribution is shown in Fig. 12. Approximately half of the s-nets (46%) are vertex-1 or vertex-2-transitive, the remaining examples embed in less symmetric fashion in $\mathbb{E}^3$, with a maximum of eight vertices per asymmetric volume. This distribution is similar to that of the vertex transitivity of the h-nets, as tile-transitive h-nets have a range of vertex transitivity, up to vertex-8-transitive examples.

3.2. Topology and ambient isotopy of epinets

The topological variety of the examples enumerated to date is broader than may be expected at first encounter with this surface reticulation technique. While low-density frameworks, such as zeolites, were the original motivation for invoking hyperbolic tessellations, we now find that high density frameworks also emerge from this process.

Table 2 reveals the distribution of s-nets with the same vertex degree (valency) at all vertices. The majority of these univalent examples are degree-four crystal nets, already studied in some detail by crystal chemists [7,33]. The *uninodal* nets that contain a single vertex per asymmetric volume are listed separately. A particularly beautiful example of a uninodal degree-5 crystal net is *sqc*1566 shown in Fig. 13.

Crystal nets of mixed degree have been explored infrequently to date. O'Keeffe lists a number in his RCSR database [13]. Table 3 lists the numbers of nets with two vertex degrees (up to a maximum degree of 12): here (3, 4) and (4, 6)-degree nets predominate. The nets included in Tables 2 and 3 comprise 80% of the enumerated s-nets *in toto*. The remaining 2832 examples contain a number of nets with mixed degrees, including

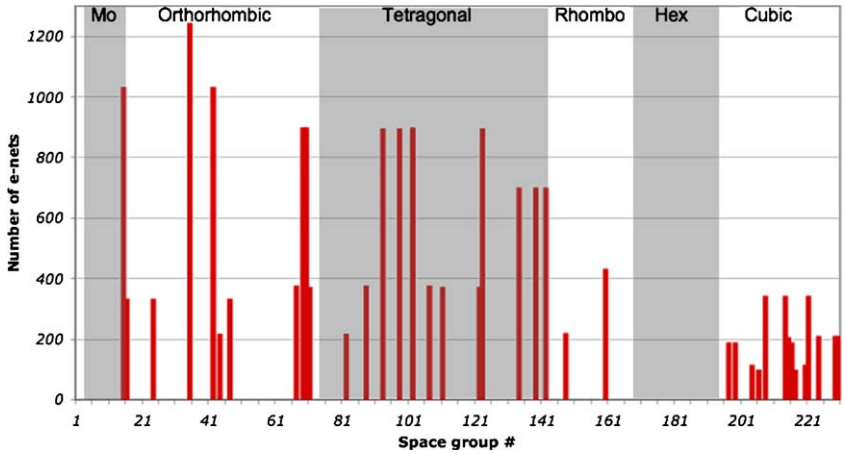

Fig. 10. Distribution of space groups of the *e*-nets formed by reticulations of the *P*, *D* and *G* three-periodic minimal surfaces. The data includes reticulations with up to two distinct tiles (and their 2D duals) with kaleidoscopic hyperbolic groups containing all side-preserving translational symmetries of the surfaces. A number of distinct embeddings of topologically identical nets are typically formed by this procedure. The space groups are those of the *e*-nets with geodesics on the surfaces. A total of $3 \times 5912 = 17736$ crystal nets are included in the histogram.

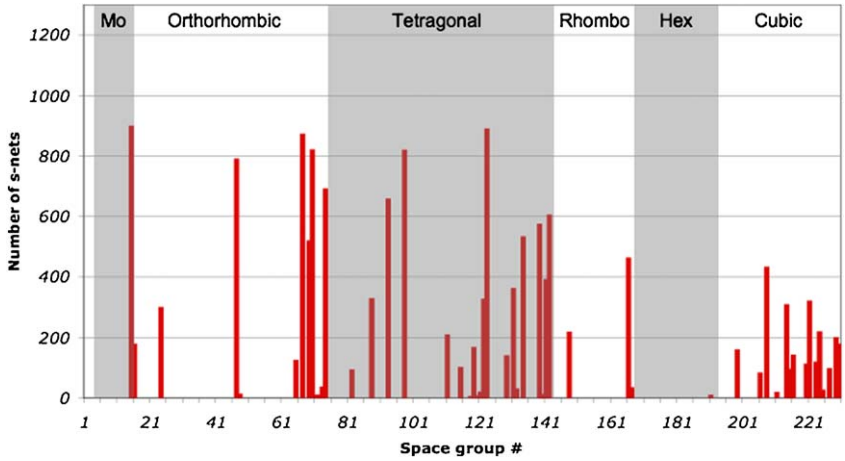

Fig. 11. Distribution of space groups of distinct barycentric embeddings of the nets collated in Fig. 10. The previous *e*-nets are filtered and reduced using the *Systre* program [17,18] to obtain 14 532 distinct crystal nets (*s*-nets).

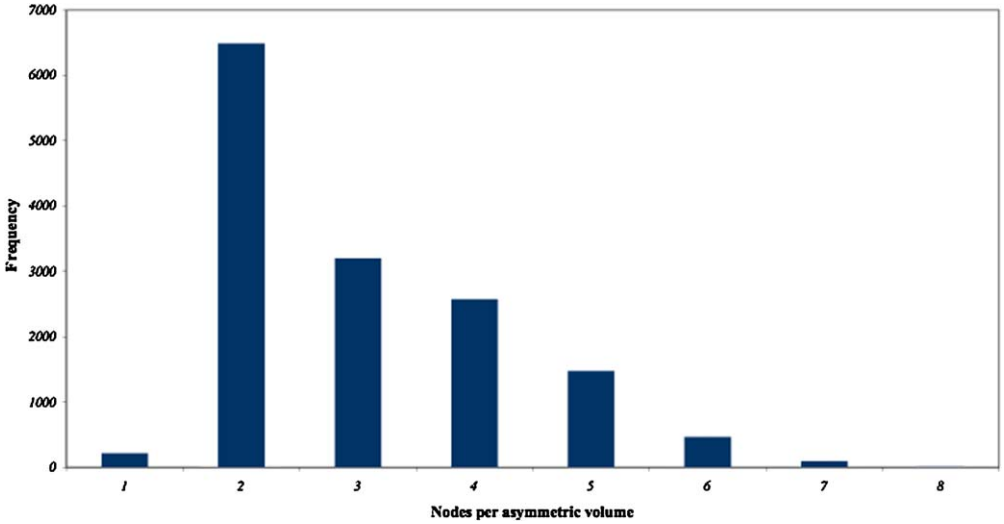

Fig. 12. Distribution of *s*-nets according to the number of distinct nodes per asymmetric volume of the relevant 3D space group.

Table 2
Numbers of univalent s-nets enumerated to date and listed in the EPINET database [27]

Degree	No. uninodal nets	No. univalent nets
3	18 (56)	155 (82)
4	46 (193)	1170 (488)
5	48 (185)	188 (187)
6	51 (159)	248 (204)
7	10 (75)	10 (77)
8	28 (40)	50 (43)
9	3 (14)	5 (14)
10	8 (15)	10 (15)
12	4 (3)	8 (7)
14	3 (1)	3 (1)
18	0 (0)	1 (0)
20	0 (0)	1 (0)

The second column collects all uninodal nets (with a single node per asymmetric volume), the third column lists all nets with all vertices of the same degree. Smaller bracketed entries list numbers of corresponding nets in the RCSR database [13].

two-valent examples with one vertex degree greater than 12, 760 examples of degrees (3, 4, 6); 724 of degrees (3, 4, 8) and 258 of degrees (4, 6, 8).

Network *coordination sequences* (also called *shell maps*) are integer sequences that capture some topological features of the net. Each term in the sequence, cs_n, describes the number of vertices accessible from a fixed vertex by a shortest walk along n edges. Our s-net data includes coordination sequences up to the tenth term, cs_{10}. This sequence (or the cumulative total of the first ten terms, td_{10}) is a useful measure of the topological density of the net—an index that correlates closely with the geometric *framework density*. It is known that coordination sequences do not offer a unique fingerprint of 3D crystal nets. For example, the zeolite frameworks RHO and LTA share the same coordination sequence [4]. Cursory inspection of coordination sequences (up to the first ten terms) indicates further difficulties in using coordination sequences as designators of net type. For example, among the very dense nets, we have found pairs of nets whose higher order terms in the sequences coincide, even for nets with distinct connectivities. An example is given in Table 4.

We have calculated coordination sequences for h-nets in addition to those of the 3D Euclidean s-nets. The collation of this data will be used to probe further the intricacies of coordination sequences. The growth rate of coordination sequences of h- and s-nets are exponential and quadratic respectively, reflecting the respective growth laws of discs with increasing radius in $\mathbb{H}^2$ and $\mathbb{E}^3$ respectively. Crystal nets may be viewed as heavily pruned and fused trees and the effect of these processes on the coefficients of quadratic growth are still poorly understood.

A particularly attractive feature of our approach is that *catenated* or *threaded* e-nets also emerge from the construction. In technical parlance, the surface reticulation procedure allows us to control the ambient isotopy of e-nets, in addition to some control over network topology via the h-net topology. A limited number of examples have been listed so far, based on simple *free* tilings of the hyperbolic plane [34]. In contrast to the Euclidean plane, *free* tiles, bounded by infinite-sided polygons, are commonplace in $\mathbb{H}^2$. The resulting h-nets are packings of disjoint hyperbolic trees, including examples that are commensurate with the PDG minimal surfaces. These examples project to $\mathbb{E}^3$ to form multi-component catenated networks [35,36]. More complex decorated trees can also be used allowing partial threading of the disjoint networks [37]. These examples suggest a far richer field of study, namely that of *knotted networks*, analogous to the closely-related knots and links of conventional knot theory. For example, edge-bridges can be inserted to connect the disjoint trees in $\mathbb{H}^2$, forming single-component h-nets. The bridging edges may be arranged so that even strong rings in the resulting e-net are threaded. The possibility of generating knotted examples is one that we are now exploring in detail [38].

4. Relevance of epinets to crystal chemistry

Our enumeration of nets to date imposes only 2D hyperbolic geometric constraints via (i) restriction to kaleidoscopic tilings of $\mathbb{H}^2$ with 1 and 2 types of tile (or vertex) and (ii) wrapping onto the P, D, and G surfaces. The aim of this research is to form a suite of crystal nets without prior regard for possible relevance to chemical frameworks, primarily to enhance our understanding of the range of crystal nets available in $\mathbb{E}^3$. The expectation is that this approach will eventually provide a complementary sample of the vast universe of 3D crystal nets to those generated by other approaches. Nevertheless, it is of interest to compare the examples derived so far with frameworks considered to be relevant to crystal chemistry. Given the continuous mutations in chemists interests in crystalline materials this is a somewhat moveable feast, but O'Keeffe and colleagues have identified crystal nets that are common to a wide variety of inorganic atomic crystals, interpenetrating networks, and MOFs (metal-organic frameworks) [39,40].

O'Keeffe's archetypes are highly symmetric nets, particularly *regular* and *semi-regular* nets [10]. Four of the five regular nets of O'Keeffe [10] are formed in our current suite of epinets: primitive cubic, *pcu* (*sqc1*)[1]; body-centred cubic, *bcu* (*sqc3*); diamond, *dia* (*sqc6*); NbO, *nbo* (*sqc35*). The fifth regular net is lattice complex $Y*$, *srs*, which is generated by wrapping a degree-3 tree onto the G surface [35]. In addition, we have generated 11 of the 15 semi-regular nets: face-centred cubic, *fcu* (*sqc19*); lattice complex vT, *lvt* (*sqc176*); sodalite, *sod* (*sqc970*); lattice complex S, *lcs* (*sqc5052*); *hxg* (*sqc947*); cristobalite, *crs* (*sqc889*); *bcs* (*sqc4991*); ReO_3, *reo* (*sqc87*); Th_3P_4, *thp* (*sqc5052*); *rhr* (*sqc5544*) and the analcime T-atom framework, *ana* (*sqc11218*). Semi-regular examples missing from EPINET are lattice complex Y, *lcy*; lattice complex V, *lcv*; *acs* and quartz, *qtz*. Among uninodal nets classified as 'important' (*srs*, *nbo*, *dia*, *pcu*, *bcu*, *ths*, *cds*) [40] only *ths* is currently missing from our enumeration. Among the 165 topologically distinct zeolite frameworks listed in the *International Zeolite Association* database [33], our current enumeration includes 17 examples among the 1000-plus s-nets of degree four.

[1] The s-net with label *sqcN* can be accessed on the web at http://epinet.anu.edu.au/sqcN.

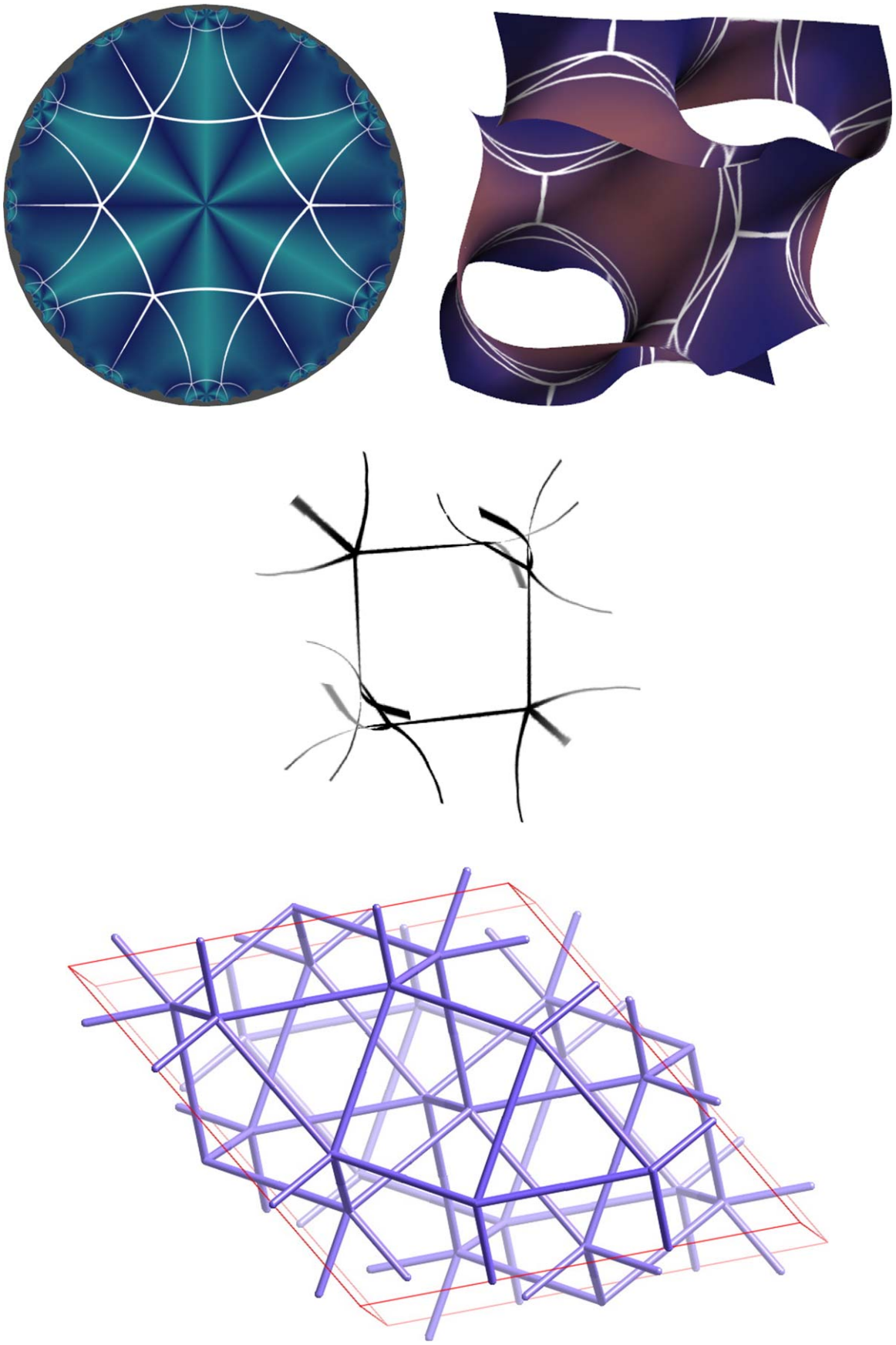

Fig. 13. The rhombohedral crystal net *sqc*1566, a novel example of a uninodal net. It results from wrapping a (12.4.6.12.4) *h*-net onto the *P* or *D* surface. We illustrate the *D* surface wrapping here. The triangles seen in the *s*-net are collar rings in the surface reticulation.

Table 3
Number of s-nets of mixed degree with two distinct vertex degrees enumerated to date in EPINET [27]

Mixed degree	4	5	6	7	8	9	10	11	12
3	2359 (27)	530 (11)	723 (10)	274 (1)	478 (1)	65 (0)	191 (0)	6 (0)	194 (0)
4		635 (9)	1473 (25)	252 (0)	1088 (2)	66 (0)	166 (0)	2 (0)	240 (2)
5			362 (2)	66 (1)	155 (0)	14 (0)	52 (0)	0 (0)	47 (0)
6				76 (0)	162 (1)	18 (0)	67 (0)	0 (0)	38 (3)
7					14 (0)	0 (0)	7 (0)	0 (0)	4 (0)
8						1 (0)	14 (0)	0 (0)	12 (0)

Smaller bracketed entries list numbers of corresponding nets in the RCSR database [13].

Table 4
Coordination sequences for distinct vertices of binodal nets *sqc*211 and *sqc*347

s-net	2D Schläfli	cs_1	cs_2	cs_3	cs_4	cs_5	cs_6	cs_7	cs_8	cs_9	cs_{10}
sqc211	$(4^4.6^2.4^4.6^2)$	12	64	168	320	520	768	1064	1408	1800	2240
	(4.6.4)	3	22	100	228	404	628	900	1220	1588	2004
sqc347	(4^{12})	12	64	168	320	520	768	1064	1408	1800	2240
	(4^4)	4	24	98	227	404	628	900	1220	1588	2004

Note that the degree-12 vertices have identical coordination sequence and that the degree-3, and -4 vertices correspond after shell 4.

Other nets of relevance to crystal chemistry enumerated so far include CdS (*sqc5*, *cds*), fluorite (*sqc169*, *flu*), γ-*Si* (*sqc2181*, *gsi*), ice II (*sqc5580*, *ict*) and ice VI (*sqc527*, *edi*), cooperite (*sqc183*, *pts*), lattice complex $S*$ (*sqc5579*, *lcs*) and pyrochlore (*sqc10956*, *pyc*).

Our goal is not merely to replicate structures already found by more conventional means, however. We find two cases of uninodal degree-3 nets, nine degree-4 examples and 29 degree-5 examples that are not already known from the RCSR database [13] or sphere-packing enumerations [31]. Some of these cases contain non-adjacent vertices (i.e., those not joined by an edge) that are closer than adjacent ones. While these cases are irrelevant as models for atomic frameworks, they are worthy candidates for more complex frameworks, such as MOFs, where these steric constraints no longer hold. Other cases are generated from h-nets that project to $\mathbb{E}^3$ to give *long edges* in their e- and s-nets, connecting to vertices in a non-adjacent unit cell. (The EPINET entry for these examples explicitly flags this feature as *Long Vectors*.) These examples—also likely to be of interest for complex molecular frameworks—are difficult to generate by conventional Euclidean crystallographic techniques as they commonly display complex threading of rings by edges.

5. Future directions

It has taken many years to set the stage for this enumeration; we expect the results to emerge rapidly from here. The immediate future is clear: we intend to enumerate non-kaleidoscopic decorations of the PDG family of surfaces. We also plan to explore reticulations of the H, CLP genus-three minimal surfaces as well as the *I-WP* (genus-four) surface. Exhaustive enumeration of free tilings of $\mathbb{H}^2$ is also on the agenda, motivated by the possibility of enumerating catenated and self-knotted crystal nets. The latter area is a particularly intriguing one. It is driven largely by crystal chemists [41], yet offers many challenges to the practising geometer!

Acknowledgements

We congratulate Hans-Georg von Schnering and apologise for remaining lost within hyperbolic geometry twenty years (and more) after we first learnt of it from Sten Andresson together with Hans-Georg. This work benefited from many discussions with Michael O'Keeffe, Davide Proserpio and Vladislav Blatov.

References

[1] A. Crum Brown, Trans. Roy. Soc. Edinburgh 23 (1864) 707–719.
[2] School of Chemistry, University of Edinburgh, Crum Brown's model of NaCl, http://www.chem.ed.ac.uk/welcome/museum_nacl.html, June 2005.
[3] A.F. Wells, Three-Dimensional Nets and Polyhedra, Wiley, New York, 1977.
[4] M. O'Keeffe, B.G. Hyde, Crystal Structures I. Patterns and Symmetry, Mineralogical Society of America, Washington, DC, 1996.
[5] O. Delgado-Friedrichs, M. O'Keeffe, J. Solid State Chem. 178 (2005) 2480–2485.
[6] S.J. Chung, Th. Hahn, W.E. Klee, Acta. Cryst. A 40 (1984) 42–50.
[7] M.M.J. Treacy, K.H. Randall, S. Rao, J.A. Perry, D.J. Chadi, Z. Krist. 212 (1997) 768–791;
See also: How the hypothetical frameworks are generated, part of the Hypothetical Zeolites project of Martin Foster and Michael Treacy, http://www.hypotheticalzeolites.net/DATABASE/Explanation.html.
[8] O. Delgado-Friedrichs, Theoret. Comput. Sci. 303 (2003) 431–445.
[9] O. Delgado-Friedrichs, A.W.M. Dress, D.H. Huson, J. Klinowski, A.L. Mackay, Nature 400 (1999) 644–647.
[10] O. Delgado-Friedrichs, M. O'Keeffe, O.M. Yaghi, Acta Cryst. A 59 (2003) 22–27;
O. Delgado-Friedrichs, M. O'Keeffe, O.M. Yaghi, Acta Cryst. A 59 (2003) 515–525.
[11] P. Pearce, Structure in Nature is a Strategy for Design, MIT Press, Cambridge, MA, 1978.
[12] H.S.M. Coxeter, The Beauty of Geometry: Twelve Essays, reprint of Twelve Geometric Essays, Dover Press, New York, 1999;
See also: M. Green, Infinite regular polyhedra, http://www.superliminal.com/geometry/infinite/infinite.htm.
[13] M. O'Keeffe, The Materials and Design Discovery Group, The reticular chemistry structure resource. Database available at http://rcsr.anu.edu.au.

[14] J.-G. Eon, J. Solid State Chem. 138 (1998) 55–65.
[15] J.-G. Eon, J. Solid State Chem. 147 (1999) 429–437.
[16] W.E. Klee, Cryst. Res. Technol. 39 (2004) 959–968.
[17] O. Delgado-Friedrichs, M. O'Keeffe, Acta Cryst. A 59 (2003) 351–360.
[18] O. Delgado Friedrichs, Generation, analysis and visualization of reticular ornaments using Gavrog, http://www.gavrog.org, July 2005.
[19] S. Andersson, Angew. Chem. 22 (1983) 69–81.
[20] S. Andersson, S.T. Hyde, H.G. von Schnering, Z. Kristallogr. 168 (1984) 1–17.
[21] W. Fischer, E. Koch, Z. Kristallogr. 183 (1988) 129–152.
[22] W. Fischer, E. Koch, Phil. Trans. R. Soc. Lond. A 354 (1996) 2105–2142.
[23] H.G. von Schnering, R. Nesper, Angew. Chem. Int. Ed. Engl. 26 (1987) 1059–1080.
[24] A.H. Schoen, Infinite periodic minimal surfaces without self-intersections, NASA Technical Note No. D-5541, 1970.
[25] A. Fogden, S.T. Hyde, Acta Cryst. A 48 (1992) 575–591.
[26] V. Robins, S. Ramsden, S.T. Hyde, Eur. Phys. J. B 39 (2004) 365–375.
[27] S. Ramsden, V. Robins, S.T. Hyde, S. Hungerford, EPINET: Euclidean patterns in non-Euclidean tilings, http://epinet.anu.edu.au, December 2005.
[28] J.H. Conway, D.H. Huson, Struct. Chem. 13 (2002) 247–256.
[29] D.H. Huson, Geom. Dedicata 47 (1993) 269–296.
[30] D.C. Palmer, CrystalMaker software version 7.0 for Mac OS X, 2005.
[31] W. Fischer, Z. Kristallogr. 138 (1973) 129–146;
W. Fischer, Z. Kristallogr. 140 (1974) 50–74.
[32] V. Robins, S. Ramsden, S.T. Hyde, Physica A 339 (2004) 173–180.
[33] International Zeolite Association, Atlas of Zeolite Framework Types. Link from http://www.iza-structure.org/databases/.
[34] V. Robins, S. Ramsden, S.T. Hyde, 2D hyperbolic tilings by infinite tiles, http://epinet.anu.edu.au/infinite_tiles.
[35] S.T. Hyde, C. Oguey, Europ. Phys. J. B 16 (2000) 613–630.
[36] S.T. Hyde, S. Ramsden, in: D. Bonchev, D.H. Rouvray (Eds.), Chemical Topology: Applications and Techniques, Gordon and Breach Science, Amsterdam, 2000, pp. 35–173.
[37] S.T. Hyde, A.-K. Larsson, T. DiMatteo, S. Ramsden, V. Robins, Austral. J. Chem. 56 (2003) 981–1000.
[38] S.T. Hyde, S. Ramsden, V. Robins, Knotted crystal nets, December 2005, in preparation.
[39] N.W. Ockwig, O. Delgado-Friedrichs, M. O'Keeffe, O.M. Yaghi, Acc. Chem. Res. 38 (2005) 176–182.
[40] O. Delgado-Friedrichs, M.D. Foster, et al., J. Sol. State Chem. 178 (2005) 2533–2554.
[41] V.A. Blatov, L. Carlucci, G. Ciani, D.M. Proserpio, Cryst. Eng. Comm. 6 (2004) 377–395;
L. Carlucci, G. Ciani, D.M. Proserpio, Coord. Chem. Rev. 246 (2003) 247–289.